

Template-based Minor Embedding for Adiabatic Quantum Optimization*

Thiago Serra¹, Teng Huang², Arvind Raghunathan³, and David Bergman²

¹Bucknell University

²University of Connecticut

³Mitsubishi Electric Research Laboratories

Abstract

Quantum Annealing (QA) can be used to quickly obtain near-optimal solutions for Quadratic Unconstrained Binary Optimization (QUBO) problems. In QA hardware, each decision variable of a QUBO should be mapped to one or more adjacent qubits in such a way that pairs of variables defining a quadratic term in the objective function are mapped to some pair of adjacent qubits. However, qubits have limited connectivity in existing QA hardware. This has spurred work on preprocessing algorithms for embedding the graph representing problem variables with quadratic terms in the hardware graph representing qubits adjacencies, such as the Chimera graph in hardware produced by D-Wave Systems. In this paper, we use integer linear programming to search for an embedding of the problem graph into certain classes of minors of the Chimera graph, which we call *template embeddings*. One of these classes corresponds to complete bipartite graphs, for which we show the limitation of the existing approach based on minimum Odd Cycle Transversals (OCTs). Some of the formulations presented are exact, and thus can be used to certify the absence of a minor embedding. On an extensive test set consisting of random graphs from five different classes of varying size and sparsity, we can embed 38% more graphs than a state-of-the-art OCT-based approach.

*Thiago Serra and Teng Huang were employed by Mitsubishi Electric Research Laboratories during the development of this project.

1 Introduction

Quantum Annealing (QA) is a technique based on a system of quantum particles in which the Hamiltonian—an operator corresponding to the sum of potential and kinetic energies—is modeled after the objective function of a binary optimization problem (Finnila et al., 1994; Kadowaki and Nishimori, 1998). Adiabatic Quantum Computation (AQC) is a particular form of QA that exploits the adiabatic theorem of quantum physics (Farhi et al., 2000, 2001), which states that a quantum system in the ground state evolves predominantly in the ground state—i.e., at the lowest possible energy level—if the rate at which the system changes is sufficiently small. Hence, AQC can approximately solve unconstrained optimization problems by slowly evolving a quantum system from a configuration in known ground state toward a configuration in which the ground state corresponds to a solution of minimum value of the optimization problem.

It is possible to model many combinatorial optimization problems with such a technique (Lucas, 2014). However, it is not known if the quantum system can always evolve in polynomial time on the inputs in order to reach a quantum speedup—i.e., solve a problem much faster than any classical algorithm would (Rønnow et al., 2014). For example, there are cases in which a linear transformation between quantum states requires exponential time (Van Dam et al., 2001).

Nevertheless, for some problems the quantum system evolves efficiently (Farhi et al., 2000) or at least faster than classical algorithms (Lucas, 2018). When compared with commercial optimization software, AQC has been found to perform better in one case (McGeoch and Wang, 2013) and comparable in another (Coffrin et al., 2019).

AQC has been used to approximately solve Quadratic Unconstrained Binary Optimization (QUBO) problems of the form

$$\min_{x \in \{0,1\}^n} x^T Q x,$$

where $Q \in \mathbb{R}^{n \times n}$ are input data and x are decision variables.¹ Without loss of generality, let Q be an upper-triangular matrix. In this paper, we will refer to any device implementing AQC as a *quantum annealer*, or a QA hardware.

While existing QA hardware may potentially be used on problems with as many as 2048 variables, in practice only problems that are much smaller

¹According to Boros and Hammer (2002), QUBO is also known as a quadratic pseudo-Boolean function in the literature since Kalantari (1986).

or substantially sparse can be directly formulated. To circumvent this limitation to some extent, we may use a surrogate formulation in which the optimal solutions can be mapped to optimal solutions of the original problem. For defining such formulation, it is often necessary to analyze the structure of the QA hardware and of the optimization problem that we want to solve. That entails solving the NP-complete problem of determining if a graph associated with the problem is a minor of a graph associated with the QA hardware.

In this paper, we show that Integer Linear Programming (ILP) can be effectively used for this preprocessing step, in which we determine how a QUBO problem can be modeled in QA hardware if the qubits have limited connectivity. We propose ILP formulations based on particular minors of the QA hardware, which we denote *template embeddings*.

We introduce the minor embedding problem for QA hardware and previous approaches in Section 2, and then contextualize our contribution in Section 3. We describe the template embeddings, their properties, and corresponding ILP formulations in Sections 4, 5, and 6. We present experimental results in Section 7 and final remarks in Section 8.

2 Background

In this section we describe the graph embedding problem associated with QA hardware, in particular with Chimera graphs, and the previous approaches to this problem.

2.1 Hardware and Problem Graphs

The quantum annealer solves the Ising formulation

$$\min_{y \in \{-1,1\}^n} y^T J y + h^T y,$$

where $J \in \mathbb{R}^{n \times n}$ and $h \in \mathbb{R}^n$ are input data and y are decision variables. Each binary variable y_i is associated with a *qubit* i , the basic unit of quantum information, and its value corresponds to the *magnetic spin* of the quantum transistor that physically implements the qubit (D-Wave Systems, 2019). The linear coefficient h_i for each variable y_i corresponds to the *bias* of qubit i . The quadratic term J_{ij} for each pair of variables y_i and y_j , if nonzero, implies the existence of a *coupler* between qubits i and j , and the value of J_{ij} represents the *strength* of the coupler. For each QUBO formulation, there is a corresponding Ising formulation for which the variables with values -1

and 1 in an optimal solution of the Ising problem correspond to variables with values 0 and 1 in an optimal solution of QUBO, which is such that the zero elements in Q are also zero in J (Choi, 2008). Hence, we may assume that matrices Q and J have the same nonzero elements.

In practice, the hardware graph has a sparse structure. Due to engineering limitations, each qubit can only be coupled with a limited set of other qubits (Choi, 2008). That implies that we can only directly solve problems with as many variables as the number of qubits if these problems follow the same sparsity structure as the QA hardware.

A QA hardware can be modeled as an undirected graph in which the vertices correspond to qubits and the edges to pairs of coupled qubits. We denote as the *hardware graph* H . Similarly, we consider a *problem graph* G in which the vertices correspond to decision variables of an Ising formulation and the edges to pairs of variables with a quadratic term in the objective function. Let $G = (V(G), E(G))$, where $V(G) := \{v_1, v_2, \dots, v_n\}$ is the set of vertices of G and $E(G)$ is a set of edges in which $\{v_i, v_j\} \in E(G)$ if $J_{i,j} \neq 0$. Similarly, let $H = (U(H), F(H))$, where vertex $u_i \in U(H)$ corresponds to qubit i and $\{u_i, u_j\} \in F(H)$ implies that qubits i and j are coupled. For convention, we will use V_i for a subset of $V(G)$ and U_i for a subset of vertices of H or any of its minors.

A problem can be directly solved in QA hardware if there is a subgraph H' of H that is *isomorphic* to G , i.e., there is a bijective mapping between the vertices of G and H' such that adjacent vertices in G are mapped to adjacent vertices in H' . However, this greatly limits the class of problems that can be solved.

The class of solvable problems can be enlarged by allowing each vertex of the problem graph G to be mapped to possibly multiple vertices in the hardware graph H . This imposes the additional requirement that qubits associated with a vertex in G have the same spin in the ground state. For example, two coupled qubits corresponding to vertices u_i and u_j can be induced to have the same spin in the ground state if J_{ij} is negative and sufficiently large in absolute value (Kaminsky and Lloyd, 2004; Kaminsky et al., 2004). In that case, those *physical* qubits define a *logical* qubit. The multiplicity of physical qubits increases the number of neighbors and make it possible to embed a graph G with higher connectivity than that present in H . More generally, we say that G can be embedded in a hardware graph H if G is a *minor* of H (Choi, 2008). A minor of a graph is any graph that can be obtained by a sequence of vertex and edge deletions as well as edge contractions (Bondy and Murty, 2008). In the example above, contracting edge $\{u_i, u_j\}$ produces a graph in which vertices u_i and u_j are replaced by a

vertex u' that is adjacent to any vertex that was originally adjacent to either u_i or u_j . Hence, the *embedding* of G in H consists of assigning each vertex $v_i \in V(G)$ to a distinct set of vertices $U_i \subseteq U(H)$ such that the induced subgraph on U_i is connected and, for each edge $\{v_i, v_j\} \in E(G)$, there exists $u_k \in U_i$ and $u_l \in U_j$ such that $(u_k, u_l) \in F(H)$.

In the QAs produced and commercially available by D-Wave Systems, the hardware graph follows the structure of a *Chimera graph*. Let us denote it as a graph $C_{M,N,L}$ such that $M \times N \times 2 \times L$ vertices are distributed in a grid of $M \times N$ cells. Each cell contains $2 \times L$ vertices. Each of those cells is a complete bipartite graph $K_{L,L}$, where a left and a right partition each contain L vertices. For ease of explanation, let us number the vertices in each partition from 1 to L . The i -th vertex in each left (right) partition is also adjacent to the corresponding i -th vertex of the left (right) partition in the cell above (to the left) and below (to the right). Figure 1 depicts $C_{2,2,4}$.

The following hardware graphs have been used in QA hardware: $C_{4,4,4}$ in D-Wave One, $C_{8,8,4}$ in D-Wave Two, $C_{12,12,4}$ in D-Wave 2X, and $C_{16,16,4}$ in D-Wave 2000Q (Dattani et al., 2019). Since $M = N$ in all cases, we will follow the convention of considering Chimera graphs of the form $C_{M,M,L}$.

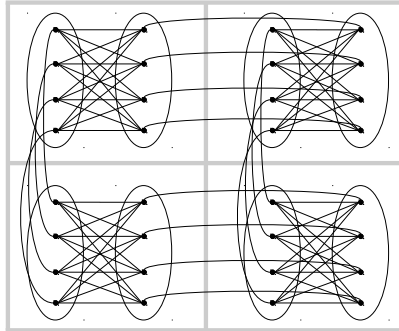


Figure 1: Chimera graph $C_{2,2,4}$ with a $K_{4,4}$ on each cell of a 2×2 grid.

2.2 Minor Embedding Algorithms

Early work on minor embedding into hardware graphs has focused on complete graphs (or *cliques*). A clique K_n is a graph on n vertices in which all vertices are adjacent to one another. If K_n can be embedded into a hardware graph H , then any other graph G with at most n vertices can be embedded in the same hardware graph H , since G is isomorphic to a subgraph of K_n .

The TRIAD algorithm was the first technique to embed cliques in hardware graphs with limited connectivity of the qubits (Choi, 2011).

The TRIAD algorithm associates each vertex of the problem graph with a chain of vertices of the hardware graph that is long enough to have at least one vertex that is adjacent to some vertex of all other chains. These chains can be embedded into a Chimera graph, where a clique $K_{L \times M}$ fits into $C_{M,M,L}$ (Choi, 2011). In fact, it is possible to embed a clique of size $LM + 1$, but no clique larger than $L(M + 1)$, in $C_{M,M,L}$ (Klymko et al., 2014). Later work in Boothby et al. (2016) generalized the form by which such clique embeddings can be obtained and consequently showed that there is an exponential number of such embeddings in the Chimera graph, which can be helpful if some qubits are inoperable and thus some vertices of the hardware graph H are missing.

Figure 2 illustrates how K_{32} can be embedded in $C_{8,8,4}$ by dividing 32 vertices into groups of 4 vertices, which are indexed from 1 to 8. The first group of 4 vertices is associated with all left partitions of the first column of unit cells and also the right partition of the bottom unit cell. The second group of 4 vertices is associated with all left partitions of the second column, except the last one, and also with the right partitions of the occupied cells in the second row from the bottom. Similar L-shaped chains follow for the remaining 6 groups. The vertices in distinct groups are adjacent to one another through the cells in the upper triangle of the grid, and the vertices within each group are adjacent to one another through the cells in the main diagonal of the grid. If we associate the remaining cells with a single additional vertex, then we can embed K_{33} instead. We know from Klymko et al. (2014) that we cannot embed K_{37} , but it is not known if cliques K_{34} , K_{35} , or K_{36} could be embedded in $C_{8,8,4}$.

Recent work by Date et al. (2019) has focused on limiting the number of qubits used when embedding graphs with at most $M \times L$ vertices. By reducing the number of qubits associated with each variable, their approach is able to obtain QUBO solutions that are closer to the optimal value. Another recent line of inquiry concerns embedding the product of graphs, which naturally arise as the problem graph of some formulations (Zaribafiyani et al., 2017). There are also other general-purpose approaches that break a QUBO problem into smaller parts, for example by decomposition (Bian et al., 2016) or fixing some variables to their likely value in optimal solutions (Karimi and Rosenberg, 2017).

The line of work that we will explore in this paper consists of embedding problem graphs with more than $M \times L$ vertices without decomposition, in particular for the case of dense problem graphs. In sparse problem graphs,

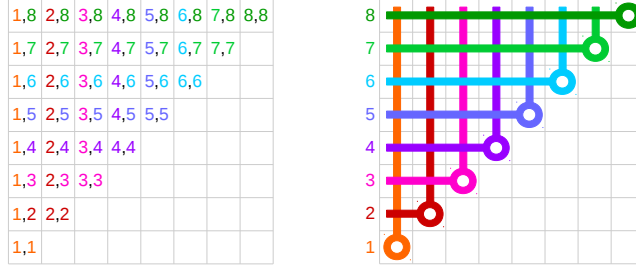


Figure 2: An embedding of K_{32} in $C_{8,8,4}$. Each group numbered from 1 to 8 consists of four connected vertices. On the left, those numbers are associated with left and right partitions of cells in the grid. On the right, vertical and horizontal lines correspond to each group occupying left and right partitions, and circles for both, following the notation in Boothby et al. (2016).

heuristics have been quite successful (Cai et al., 2014; Yang and Dinneen, 2016). Among those, one of the most widely used is the CMR algorithm (Cai et al., 2014). In dense problem graphs, the state-of-the-art consists of using a virtual hardware as an intermediary for the embedding. The virtual hardware consists of a particular minor of the Chimera graph $C_{M,M,L}$, which is chosen to preserve the ability to embed large and dense graphs while making it easy to describe the family of minors that can be obtained from it. This idea was pioneered by Goodrich et al. (2018b) with a complete bipartite graph $K_{ML,ML}$ as virtual hardware.

Figure 3 illustrates how $K_{64,64}$ can be embedded in $C_{16,16,4}$: each group of 4 vertices is associated with all right partitions of a given row or with all left partitions of a given column.

Any minor of $K_{ML,ML}$ is isomorphic to a subgraph of one among ML minors of $K_{ML,ML}$ (Hamilton and Humble, 2017). In essence, each vertex $v_i \in V(G)$ is assigned to vertices in either one or both partitions of $H = K_{ML,ML}$ to obtain an embedding of G , and thus edge $\{u_j, u_k\} \in F(H)$ is contracted if vertex v_i is assigned to both u_j and u_k .

The premise in Goodrich et al. (2018b) is to assign vertices of an Odd Cycle Transversal (OCT) of the problem graph to vertices in both partitions of $K_{ML,ML}$. An OCT of a graph G is a set T containing vertices from every odd cycle of G , hence implying that the removal of T results in a bipartite graph, and consequently the remaining vertices are each assigned to a single vertex of $K_{ML,ML}$. Those authors observed that an OCT of G having minimum size implies the minimum size of a complete bipartite graph in which G can be embedded. If T is such a minimum size OCT and

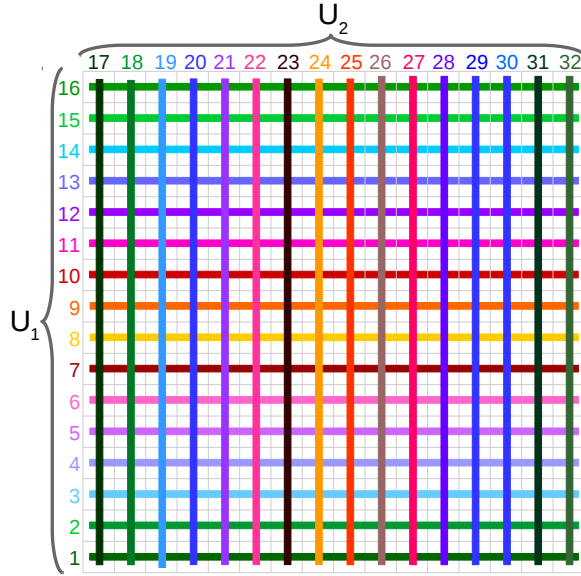


Figure 3: An embedding of $K_{64,64}$ in $C_{16,16,4}$ using groups of 4 vertices, the first 16 are associated with the right partitions of cells in each row (set U_1) and the last 16 with the left partitions of cells in each column (set U_2).

V_1 and V_2 are the resulting partitions of the subset of vertices defined by $V(G) \setminus T$, then it follows that G can only be embedded in complete bipartite graphs having at least $2|T| + |V_1| + |V_2|$ vertices.

Later work in Goodrich et al. (2018a) used ILP formulations to find an OCT of minimum size, hence minimizing $|T|$ as an approach to determine if a given problem graph is embeddable in $K_{ML,ML}$. They report that customized algorithms can find an OCT of smaller graphs faster. However, they also acknowledge that a general-purpose solver is more effective in cases where the problem graphs are harder to embed. We argue in this paper that an OCT of minimum size is not a certificate of embeddability.

2.3 Related Work

A group of authors has been exploring how to solve a broader class of optimization problems with QA hardware. Recent work by Dridi et al. (2018) uses Groebner bases to represent optimization problems involving polynomial functions of higher order on binary domains as QUBO problems, which can then potentially be solved by existing QA hardware. Subsequent work by Alghassi et al. (2019) uses Graver bases to achieve the same with integer

non-linear optimization problems, which may also include constraints.

One can also solve a QUBO using integer linear programming, since the quadratic terms on binary variables can be linearized with an extended formulation (Padberg, 1989). In recent work, Coffrin et al. (2019) uses ILP to verify the solutions generated by QA hardware.

3 Contributions of This Paper

We show how Integer Linear Programming (ILP) can be used as an effective preprocessing step in AQC, especially for problem graphs with more vertices than the largest embeddable cliques. Note that we are not interested in solving minor embedding problems that could be nearly as difficult as the corresponding QUBO problem. We focus instead on how classical optimization algorithms could leverage the potential of quantum optimization algorithms. Hence, we strive for a balance between computational speed and the ability to embed larger problem graphs by defining simple formulations that exploit the structure of Chimera graphs. In each of these formulations, we cluster the vertices of a minor of the Chimera graph in some partitions and formulate a problem of deciding how to assign vertices of the problem graph to one or more of such partitions. In summary, our main contributions are:

- (i) We propose Template Embeddings (TEs) as a generalization of the virtual hardware concept. Each template embedding is a minor of the Chimera graph that can embed a variety of problem graphs with few edge contractions. We study three classes of those: the Bipartite TE (BTE), as the virtual hardware in Goodrich et al. (2018b); the Quadripartite TE (QTE); and the Clique Overlap TE (COTE).
- (ii) We show that the current approach of finding an OCT of minimum size cannot certify that a given problem graph cannot be embedded in BTE.
- (iii) We present ILP formulations to determine how to embed a problem graph on the minor of each template embedding with competitive results. For BTE and COTE, the formulation provides a certificate of embeddability or lack thereof.

4 Bipartite Template Embedding

For a Chimera graph $C_{M,M,L}$, BTE consists of the minor $K_{ML,ML}$ used as virtual hardware by Goodrich et al. (2018b), in which the vertices of the hardware graph are partitioned into sets U_1 and U_2 of size ML each. The construction of BTE is described in Figure 3.

In order to embed a problem graph G in BTE, we need to determine which vertices of $V(G)$ should be assigned to partitions U_1 and U_2 . A vertex assigned to a single partition should only be adjacent to vertices assigned to the other partition. If assigning all vertices is proven impossible, then G cannot be embedded in BTE. If all vertices are assigned to at least one partition, then the solution defines a valid embedding.

Before formulating the embeddability of a problem graph G in BTE, we show that the approach in Goodrich et al. (2018b) of assigning to both partitions U_1 and U_2 only the vertices of G in an OCT of minimum size does not suffice in some cases.

4.1 OCTs and Bipartite Embedding

In this section, we characterize the relationship between OCTs of a graph G and the embedding of G in a complete bipartite graph K_{m_1,m_2} . More specifically, we show that:

- (i) The set of vertices $S \subseteq V(G)$ that are assigned to both partitions of K_{m_1,m_2} in any embedding of G is a superset of some OCT $T \subset V(G)$, but T may be a proper subset of S in each of the possible embeddings.
- (ii) The largest OCT T contained in S may not be an OCT of minimum size in any of the possible embeddings.

Those results are shown in the following propositions.

Proposition 1. *For any embedding of a graph G in K_{m_1,m_2} , the set of vertices $S \subseteq V(G)$ assigned to both partitions of K_{m_1,m_2} is such that there is an OCT T of G for which $T \subseteq S$. In some cases, $T \subset S$ in every possible embedding.*

Proof. First we show that the set of vertices S assigned to both partitions in any embedding is a superset of an OCT T . Let us suppose, for contradiction, that none of the vertices incident to an odd cycle of G are in S , say $v_1v_2 \dots v_kv_1$ for $k \geq 3$ and odd. Since each of those vertices is assigned to one partition of K_{m_1,m_2} , whereas consecutive vertices should necessarily be

in different partitions, then one partition is assigned to each v_i with even i and the other partition is assigned to each v_i with odd i . However, since v_k and v_1 are adjacent and assigned to the same partition, then we do not have a valid embedding, and we reach a contradiction. Hence, S contains at least one vertex of every odd cycle in G and is indeed an OCT. This proves the first claim.

Next we show that the embedding of certain graphs implies that we assign to both partitions a vertex that is not incident to any odd cycle. In particular, let us consider a *star graph* $K_{1,m}$, where a single vertex v is adjacent to all the other vertices and consequently the only OCT is an empty set. If $m > \max\{m_1, m_2\}$ but $m \leq m_1 + m_2 - 2$, then we can only embed $K_{1,m}$ in K_{m_1, m_2} if vertex v is assigned to both partitions, in which case each of the remaining m vertices can then be assigned to either partition of K_{m_1, m_2} . \square

Proposition 2. *There is a graph G that can be embedded in K_{m_1, m_2} , where the set of vertices $S \subseteq V(G)$ assigned to both partitions of K_{m_1, m_2} that are incident to odd cycles in any such embedding is not an OCT of minimum size.*

Proof. Let us consider a graph G in which $V(G) := \{v_1, v_2, v_3\} \cup V_A \cup V_B$, where vertices v_1 and v_2 are adjacent and each is also adjacent to all vertices in set V_A , whereas v_3 is adjacent to all vertices in sets V_A and V_B , and there are no other edges in G (see Figure 4 for an example). Vertices v_1 and v_2 define cycles of size 3 with every vertex in V_A , and removing either of them makes the graph bipartite. Thus, the OCTs of minimum size in G are $\{v_1\}$ and $\{v_2\}$.

The graphs resulting from removing either such OCT from G are isomorphic. Without loss of generality, let us remove v_1 . In that case, vertex v_2 and the vertices in set V_A are necessarily in different partitions. Since vertex v_3 is adjacent to the vertices in V_A , it follows that v_3 is in the same partition as v_2 . Since the vertices in V_B are all adjacent to v_3 , then the vertices in V_B are in the same partition as those in V_A . Consequently, the graph obtained by removing $\{v_1\}$ has a partition $\{v_2, v_3\}$ of size 2 and another partition $V_A \cup V_B$ of size $|V_A| + |V_B|$. Therefore, we can only embed graph G in K_{m_1, m_2} by assigning the vertices in a minimum size OCT to both partitions and the rest to a single partition each if $m_1 \geq 3$ and $m_2 \geq |V_A| + |V_B| + 1$ or vice-versa.

Assuming $|V_A| \geq 2$, let $v_4 \in V_A$ and $v_5 \in V_A$ be a pair of distinct vertices, which are in the odd cycle $v_3v_4v_1v_2v_5v_3$. If we remove OCT $\{v_1, v_3\}$ from

G , then vertex v_2 and the vertices in V_A are again in different partitions. Since the vertices in V_B are not adjacent to the other remaining vertices, then one possible partitioning of the remaining vertices is $\{v_2\} \cup V_B$ and V_A , hence implying that we can embed G in K_{m_1, m_2} if $m_1 \geq |V_B| + 3$ and $m_2 \geq |V_A| + 2$ or vice-versa.

If $m_1 = m_2 = 64$ and $|V_A| = |V_B| = 32$, as in Figure 4, then assigning only the vertices of a minimum size OCT $\{v_1\}$ to both partitions and assigning $V_A \cup V_B$ to a single partition is not feasible since no partition has 65 ($= |V_A \cup V_B \cup \{v_1\}|$) vertices. However, it is possible to assign only the vertices of the OCT $\{v_1, v_3\}$ to both partitions and obtain an embedding, since in such case we only need to assign 35 ($= |\{v_2\} \cup V_B \cup \{v_1, v_3\}|$) vertices to one partition of K_{m_1, m_2} and 34 ($= |V_A \cup \{v_1, v_3\}|$) vertices to the other. \square

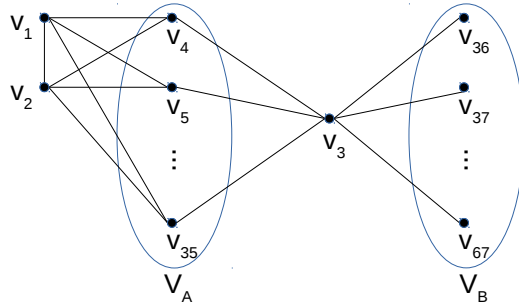


Figure 4: Illustration for the proof of Proposition 2.

In summary, the set of vertices that should be assigned to both partitions of K_{m_1, m_2} is a superset of an OCT, but it may contain vertices that are not incident to odd cycles (Proposition 1). When those vertices are removed, the resulting set may not be an OCT of minimum size (Proposition 2). Hence, the embedding approach in Goodrich et al. (2018b) may fail to embed graphs that are embeddable using BTE.

The rationale for finding an OCT T of minimum size is that it allows G to be embedded in the smallest complete bipartite graph, regardless of the size of each partition in which we are embedding. However, the size of the partitions matter. If we denote the partitions of $G \setminus T$ as the sets of vertices V_1 and V_2 , then G can only be embedded with such partitions in K_{m_1, m_2} if $\min(m_1, m_2) \geq |T|$ and $\max(m_1, m_2) \geq |T| + |V_1| + |V_2|$. The graph in Figure 4 can be embedded with an OCT of minimum size in $K_{3, 65}$, which has only 68 vertices. It can also be embedded with a larger OCT in $K_{34, 35}$, which has 69 vertices. For a Chimera graph $C_{16, 16, 4}$, only the second

embedding above would be possible in BTE.

4.2 Exact Bipartite Embedding

The formulation below determines if a problem graph G is embeddable in BTE.

Decision Variables For each vertex $v_i \in V(G)$ and $k \in \{1, 2\}$, let $y_{i,k} \in \{0, 1\}$ be a binary variable for whether vertex v_i is assigned to partition U_k and let $y'_i \in \{0, 1\}$ be a binary variable denoting whether v_i is assigned to any partition.

Objective Function The following expression aims at assign as many vertices as possible:

$$\max \sum_{i=1}^n y'_i.$$

If the ILP solver reports an upper bound lower than n , then it is not possible to embed G in BTE.

Constraints For each vertex $v_i \in V(G)$, we associate both types of decision variables as follows:

$$y'_i \leq y_{i,1} + y_{i,2}.$$

For each partition U_k , $k \in \{1, 2\}$, no more than ML vertices of $V(G)$ should be assigned to it:

$$\sum_{i=1}^n y_{i,k} \leq M \times L.$$

For each edge $\{v_i, v_j\} \in E(G)$, $i < j$, vertices v_i and v_j should not be assigned to a single and same partition:

$$y_{i,1} + y_{j,1} - y_{i,2} - y_{j,2} \leq 1$$

$$y_{i,2} + y_{j,2} - y_{i,1} - y_{j,1} \leq 1.$$

The constraints above are the canonical cuts on the unit hypercube defined by the binary variables (Balas and Jeroslow, 1972). Each corresponds to the tightest single inequality on such space because it separates a single

combination of values for those variables and is tight for each combination of values that differs in only one variable. For example, the first inequality above separates $(y_{i,1}, y_{i,2}, y_{j,1}, y_{j,2}) = (1, 0, 1, 0)$ from the feasible set while holding at equality for the adjacent assignments $(y_{i,1}, y_{i,2}, y_{j,1}, y_{j,2}) = (0, 0, 1, 0), (1, 1, 1, 0), (1, 0, 0, 0),$ and $(1, 0, 1, 1)$.

Proposition 3 (Certificate of Embeddability). *Graph G is embeddable in BTE if and only if there is a solution to the ILP formulation with objective value $|V(G)|$.*

The claim is easily proven, and we omit it for sake of brevity. An important implication is that we can terminate the search process and conclude that G is not embeddable in BTE once the search determines that there is no solution with objective value $|V(G)|$. Search algorithms incorporate a number of domain reduction techniques, which lead to considerable pruning of the search space, and this can be favorably exploited to produce a certificate of non-embeddability. Furthermore, any solution with objective value $|V(G)|$ is an optimal solution, and the search can be terminated if one of those is found.

5 Quadripartite Template Embedding

We define the Quadripartite Template Embedding (QTE) as a minor of the Chimera graph with vertices partitioned into sets $U_1, U_2, U_3,$ and U_4 . Each vertex in U_1 is adjacent to all vertices in U_2 , those in U_2 are also each adjacent to a distinct vertex in U_3 , and those in U_3 are also adjacent to all vertices in U_4 . In other words, the subgraph induced on $U_1 \cup U_2$ and $U_3 \cup U_4$ are both complete bipartite graphs, and the subgraph induced in $U_2 \cup U_3$ is a perfect matching. In fact, embedding on QTE generalizes embedding on BTE, since BTE is a minor of QTE after contracting all edges between sets U_2 and U_3 : $U_1 \cup U_4$ defines one partition of BTE in that case and the other partition is defined by the vertices resulting from contracting the edges between U_2 and U_3 . For a Chimera graph $C_{M,M,L}$ with M even and thus $P := M/2$ integer, the size of those partitions are: $|U_1| = PL, |U_2| = ML, |U_3| = ML,$ and $|U_4| = PL$. Figure 5 illustrates that minor of $C_{16,16,4}$.

QTE can be obtained from $C_{M,M,L}$ as follows. Set U_1 consists of P groups of L vertices, each group obtained by contracting the L vertices of the right partitions of one of the top P rows of the $M \times M$ grid. Set U_2 consists of M groups of L vertices, each group obtained by contracting the L vertices of the left partitions in the top P rows of one of the M columns

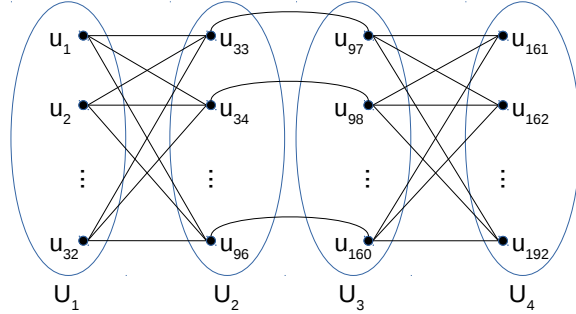


Figure 5: QTE minor of Chimera graph $C_{16,16,4}$.

of the grid. Set U_3 consists of M groups of L vertices, each group obtained by contracting the L vertices of the left partitions in the bottom P rows of one of the M columns of the grid. Set U_4 consists of P groups of L vertices, each group obtained by contracting the L vertices of the right partitions of one of the bottom P rows of the grid. Figure 6 illustrates QTE in $C_{16,16,4}$.

In order to embed a problem graph in QTE, each vertex should be assigned to a sequence of adjacent partitions and each pair of adjacent vertices v_i and v_j should be assigned to vertices u_i and u_j that are adjacent in QTE. For simplicity, we only consider u_i and u_j to be adjacent for satisfying the later criterion if they are in distinct partitions that together induce a complete bipartite graph, i.e., U_1 and U_2 or U_3 and U_4 . Hence, we ignore the possibility of assuming u_i and u_j adjacent if one of these vertices is in partition U_2 and the other vertex is in partition U_3 . Otherwise, we would need to explicitly assign the vertices of the problem graph to specific vertices in those partitions instead of merely deciding that the vertices of the problem graph are assigned to some vertex in the partition, which would make the formulation considerably more complex. Given our aim for simplicity, the formulation below does not provide a certificate of embeddability in QTE.

Decision Variables For each vertex $v_i \in V(G)$ and $k \in \{1, 2, 3, 4\}$, let $y_{i,k} \in \{0, 1\}$ be a binary variable for whether vertex v_i is assigned to partition U_k , and let $y'_i \in \{0, 1\}$ be a binary variable denoting whether v_i is assigned to any partition. For each edge $\{v_i, v_j\} \in E(G)$, assuming $i < j$, let $z_{i,j}^k \in \{0, 1\}$ be an auxiliary binary variable implying that the adjacency between vertices v_i and v_j is ensured by assigning vertex v_i to partition U_k and vertex j to the partition in which all vertices are adjacent to those in U_k .

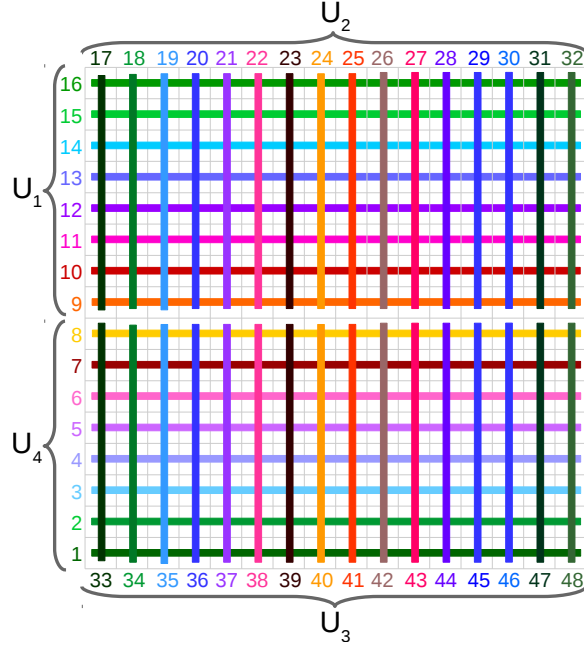


Figure 6: QTE in $C_{16,16,4}$, defining partition U_1 with the top 8 horizontal groups, U_2 with the top 16 vertical groups, U_3 with the bottom 16 vertical groups, and U_4 with the bottom 8 horizontal groups. Each group has 4 vertices.

Objective Function We maximize vertices assigned:

$$\max \sum_{i=1}^n y'_i.$$

Constraints The first constraint associates the first two types of variables for each vertex $v_i \in V(G)$, as in BTE:

$$y'_i \leq \sum_{k=1}^4 y_{i,k}.$$

For each partition U_k , $k \in \{1, 2, 3, 4\}$, the number of vertices assigned to U_k is bounded by the size of that partition:

$$\sum_{i=1}^n y_{i,k} \leq |U_k|.$$

For each vertex $v_i \in V(G)$, we want the set of partitions to which v_i is assigned to be pairwise contiguous. We formulate that with constraints preventing each possible discontinuity: (i) assigning v_i to U_1 and U_3 implies that v_i is also assigned to U_2 ; (ii) assigning v_i to U_1 and U_4 implies that v_i is also assigned to U_2 and U_3 ; and (iii) assigning v_i to U_2 and U_4 implies that v_i is also assigned to U_3 . Hence, we use canonical cuts on the unit hypercube in the corresponding subspaces to exclude the assignments $(y_{i,1}, y_{i,2}, y_{i,3}) = (1, 0, 1)$ for (i); $(y_{i,1}, y_{i,2}, y_{i,4}) = (1, 0, 1)$ and $(y_{i,1}, y_{i,3}, y_{i,4}) = (1, 0, 1)$ for (ii); and $(y_{i,2}, y_{i,3}, y_{i,4}) = (1, 0, 1)$ for (iii):

$$\begin{aligned} y_{i,1} + y_{i,3} - y_{i,2} &\leq 1 \\ y_{i,1} + y_{i,4} - y_{i,2} &\leq 1 \\ y_{i,1} + y_{i,4} - y_{i,3} &\leq 1 \\ y_{i,2} + y_{i,4} - y_{i,3} &\leq 1. \end{aligned}$$

For (ii), it would suffice to exclude $(y_{i,1}, y_{i,2}, y_{i,3}, y_{i,4}) = (1, 0, 0, 1)$ with $y_{i,1} + y_{i,4} - y_{i,2} - y_{i,3} \leq 1$ because the other cases are covered. However, by summing the two inequalities used for (ii) we obtain the implied inequality $2y_{i,1} + 2y_{i,4} - y_{i,2} - y_{i,3} \leq 2$, which is stronger than $y_{i,1} + y_{i,4} - y_{i,2} - y_{i,3} \leq 1$ on continuous domains in $[0, 1]$ and excludes additional fractional values such as $(y_{i,1}, y_{i,2}, y_{i,3}, y_{i,4}) = (1, 0.5, 0.5, 1)$. Note that a formulation that has a smaller feasible set when the binary variables on $\{0, 1\}$ are relaxed to continuous variables on $[0, 1]$ is considered as stronger and often is solved faster.

For each edge $\{v_i, v_j\} \in E(G)$, $i < j$, we want vertex v_i assigned to at least one partition U_k such that vertex v_j is assigned to the corresponding partition U_l where the set of vertices $U_k \cup U_l$ induces a complete bipartite graph. In other words, we want v_i and v_j respectively assigned to either (i) U_1 and U_2 ; (ii) U_2 and U_1 ; (iii) U_3 and U_4 ; or (iv) U_4 and U_3 :

$$\begin{aligned} y_{i,1} &\geq z_{i,j}^1, & y_{j,2} &\geq z_{i,j}^1 \\ y_{i,2} &\geq z_{i,j}^2, & y_{j,1} &\geq z_{i,j}^2 \\ y_{i,3} &\geq z_{i,j}^3, & y_{j,4} &\geq z_{i,j}^3 \\ y_{i,4} &\geq z_{i,j}^4, & y_{j,3} &\geq z_{i,j}^4 \\ \sum_{k=1}^4 z_{i,j}^k &\geq 1. \end{aligned}$$

Note that the first two inequalities above imply $y_{i,1} + y_{j,2} \geq 2z_{i,j}^1$, which alone would also be a valid formulation for (i), and the same follows for conditions (ii), (iii), and (iv). However, having a pair of inequalities instead makes the formulation stronger since it excludes fractional solutions such as $(y_{i,1}, y_{j,2}, z_{i,j}^1) = (0.5, 0.5, 1)$. Those constraints also imply that each vertex incident to at least one edge should be assigned to a partition, and thus a non-embeddable problem graph may lead to an infeasible solution.

6 Clique Overlap Template Embedding

We define the Clique Overlap Template Embedding (COTE) as a minor of a Chimera graph with vertices partitioned into sets U_1 , U_2 , and U_3 . The subgraphs on $U_1 \cup U_2$ and $U_2 \cup U_3$ induce cliques, and there are no edges between the vertices in U_1 and U_3 . For a Chimera graph $C_{M,M,L}$ and a parameter $P \in \{1, 2, \dots, \frac{M}{2} - 1\}$, we define $\text{COTE}(P)$ with $|U_1| = (P + 1)L$, $|U_2| = (M - P - 1)L$, and $|U_3| = PL$. Figure 7 illustrates the $\text{COTE}(7)$ minor of $C_{16,16,4}$.

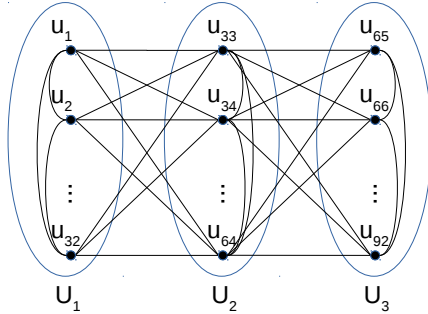


Figure 7: $\text{COTE}(7)$ minor of Chimera graph $C_{16,16,4}$.

$\text{COTE}(P)$ can be obtained from $C_{M,M,L}$ as follows. The union of sets U_1 and U_2 defines a clique of size ML in the way previously illustrated in Figure 2, which uses the main diagonal of the $M \times M$ grid and the cells above it. Let the top $P + 1$ groups correspond to set U_1 and the bottom $M - P - 1$ groups correspond to set U_2 . Set U_3 defines a clique of size PL having a mirrored construction with the next diagonal of the grid after the main diagonal and the cells to the right and below it. By extending the groups corresponding to set U_3 downward in the grid and those corresponding to set U_2 to the right, we make all the vertices in those groups adjacent. Note that some vertices in U_1 are adjacent to some vertices in U_3 , but we ignore such

edges for simplicity and define the minor without them. Figure 8 illustrates how COTE(7) is obtained from $C_{16,16,4}$.

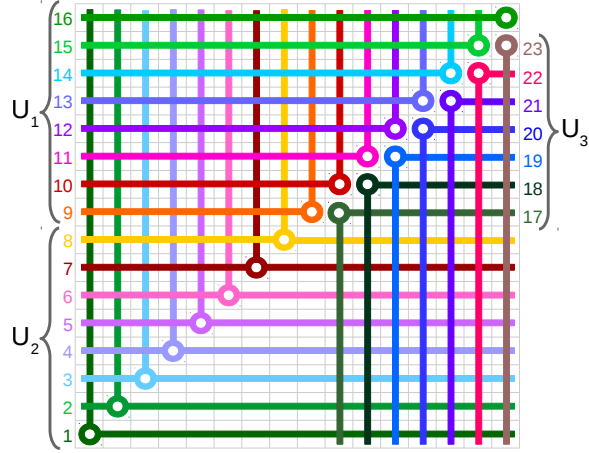


Figure 8: COTE(7) in $C_{16,16,4}$, defining partition U_1 with groups 9 to 16, partition U_2 with groups 1 to 8, and partition U_3 with groups 17 to 23. Each group has 4 vertices.

In order to embed a problem graph in COTE, it suffices for each vertex to be assigned to a single partition, since otherwise they are necessarily assigned to U_2 , and the vertices in U_2 are adjacent to all other vertices. Consequently, pairs of adjacent vertices cannot be assigned one to partition U_1 and another to U_3 .

Decision Variables For each vertex $v_i \in V(G)$ and $k \in \{1, 2, 3\}$, let $y_{i,k} \in \{0, 1\}$ be a binary variable for whether vertex v_i is assigned to partition U_k .

Objective Function We maximize vertices assigned:

$$\max \sum_{i=1}^n \sum_{k=1}^3 y_{i,k}.$$

Constraints For each vertex $v_i \in V(G)$, we should assign at most one partition:

$$\sum_{k=1}^3 y_{i,k} \leq 1.$$

For each partition U_k , $k \in \{1, 2, 3\}$, the number of vertices assigned to U_k is bounded by the size of that partition:

$$\sum_{i=1}^n y_{i,k} \leq |U_k|.$$

For each edge $\{v_i, v_j\} \in E(G)$, $i < j$, vertex v_i cannot be assigned to U_1 if v_j is assigned to U_3 and vice-versa:

$$y_{i,1} + y_{j,3} \leq 1$$

$$y_{i,3} + y_{j,1} \leq 1.$$

Proposition 4 (Certificate of Embeddability). *Graph G is embeddable in COTE if and only if there is a solution to the ILP formulation with objective value $|V(G)|$.*

The comments following Proposition 3 also hold for COTE.

7 Experiments

We implemented the ILP formulations for the template embeddings in $C_{16,16,4}$ using Gurobi 8.0.0. We compare our results with those obtained with fast-ort-reduce (FOR) using the source code from Goodrich et al. (2018b). We use five random generators of graphs with a density parameter $p = .25$ for Low density, $p = .5$ for Medium density, and $p = .75$ for High density. Four generators are from Goodrich et al. (2018b): Barabási-Albert, Erdős-Rényi, Regular, and Noisy Bipartite. We implement Percolation based on long-range percolation graphs (Coppersmith et al., 2002). For each vertex v_i , we draw a random number $\chi_i \in [0, 1)$ and we include edge $\{v_i, v_j\}$ with probability $\min\left\{1, \frac{p}{|\chi_i - \chi_j|}\right\}$.

Since TRIAD can easily generate a clique of size 64 for $C_{16,16,4}$, we generate 5 random graphs from each generator and with each density for number of vertices ranging from 65 to 128. The time required to embed problems is currently the bottleneck in solving problems on QA hardware. With an eye towards reducing this time, we set a tight time limit of 15 seconds for each algorithm on each graph. All experiments were conducted on a single thread in an Intel(R) Core(TM) i7-3930K CPU @ 3.20GHz with 32GB of RAM.

Figure 9 shows the total number of embedded graphs per algorithm. Figure 10 shows the total number of graphs that are uniquely embedded by

different templates. Table 1 shows the largest graph that each algorithm could embed within the time limit for each random generator and density, with the largest numbers of each row in bold. Table 2 shows the number of graphs embedded by each approach per random graph model and in total.

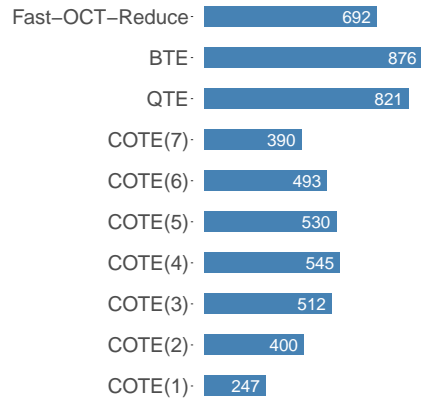


Figure 9: Number of graphs embedded by Fast-OCT-Reduce and any template embedding.

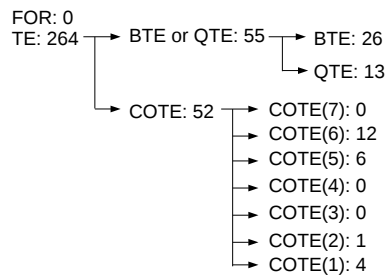


Figure 10: Graphs uniquely embedded by a family or a specific type of template embedding.

Table 1: The largest graph embedded by each algorithm per generator and density.

Random Graph	Density	FOR	BTE	QTE	COTE(7)	COTE(6)	COTE(5)	COTE(4)	COTE(3)	COTE(2)	COTE(1)
Percolation	Low	67	68	67	65	65	65	66	67	69	68
	Medium	66	66	66	—	—	—	—	65	65	65
	High	66	66	66	—	—	—	—	—	—	—
Barabási-Albert	Low	78	78	76	68	69	71	73	74	72	68
	Medium	71	72	71	65	66	66	67	68	69	68
	High	69	69	68	—	65	65	65	65	66	66
Erdős-Rényi	Low	79	80	79	69	71	72	74	76	72	68
	Medium	71	72	71	65	66	67	67	68	69	68
	High	69	69	68	—	—	65	65	65	66	67
Regular	Low	78	89	95	87	88	84	80	76	72	68
	Medium	72	82	85	88	88	84	80	76	72	68
	High	69	79	81	85	88	84	80	76	72	68
Noisy Bipartite	Low	92	92	90	74	76	80	80	76	72	68
	Medium	85	85	82	68	70	73	79	76	72	68
	High	81	81	76	66	69	69	73	76	72	68

Table 2: Number of graphs embedded by each approach.

Random Graph	Fast-OCT-Reduce	Template Embeddings
Percolation	35	41
Barabási-Albert	113	126
Erdős-Rényi	128	139
Regular	126	350
Noisy Bipartite	290	300
Total	692	956

Analysis The ILP formulations based on template embeddings can embed 38% more graphs than the OCT-based approach. Furthermore, every graph embedded by the OCT-based approach is also embedded by one of the template embeddings. The results are particularly favorable with regular graphs. While BTE is a special case of QTE, the simpler formulation allowed BTE to embed more Barabási-Albert, Erdős-Rényi, and Noisy Bipartite graphs within the time limit. QTE and COTE performed comparatively better with Percolation and Regular graphs in alternate densities.

8 Conclusion and Future Work

We proposed the concept of template embeddings to map quadratic unconstrained binary optimization problems in quantum annealers. Each template embedding corresponds to a minor of the Chimera graph that can embed a variety of large and dense graphs. We also introduced integer linear programming formulations to find such mappings and showed that two of these formulations are exact, and thus certify if a given graph can be embedded in the corresponding minor. Experimental results clearly demonstrate the potential of the proposed approach, especially to embed problems having more variables than the maximum embeddable clique in the Chimera graph corresponding to the QA hardware.

Interestingly, our approach makes a better use of quantum annealers by leveraging classical optimization algorithms as a preprocessing step. The performance of solvers for mixed-integer linear programming has improved by orders of magnitude in the past decades (Bixby, 2012). We believe that there is potential for further coordination between classical and quantum algorithms for discrete optimization.

In future work, we intend to investigate template embeddings that are

adaptive to problem sparsity and incorporate knowledge of faulty qubits in the formulations. We also aim to extend the template-based approach to minors of Pegasus, the proposed hardware graph for future QA hardware by D-Wave Systems (Dattani et al., 2019).

Acknowledgements The authors would like to thank Claudio Leonardo Lucchesi and Yoshiharu Kohayakawa for their input on random graphs.

References

- Hedayat Alghassi, Raouf Dridi, and Sridhar Tayur. Graver bases via quantum annealing with application to non-linear integer programs. *arXiv*, abs/1902.04215, 2019.
- E. Balas and R. G. Jeroslow. Canonical cuts on the unit hypercube. *SIAM Journal on Applied Mathematics*, 23:61–69, 1972.
- Zhengbing Bian, Fabian Chudak, Robert Brian Israel, Brad Lackey, William G. Macready, and Aidan Roy. Mapping constrained optimization problems to quantum annealing with application to fault diagnosis. *Frontiers in ICT*, 3:14, 2016.
- Robert E. Bixby. A brief history of linear and mixed-integer programming computation. In *Documenta Mathematica, Extra Volume: Optimization Stories*, pages 107–121. 2012.
- J. A. Bondy and U. S. R. Murty. *Graph Theory*. Springer, 2008.
- Tomas Boothby, Andrew D King, and Aidan Roy. Fast clique minor generation in chimera qubit connectivity graphs. *Quantum Information Processing*, 15(1):495–508, 2016.
- Endre Boros and Peter L Hammer. Pseudo-boolean optimization. *Discrete applied mathematics*, 123(1-3):155–225, 2002.
- J. Cai, W. G. Macready, and A. Roy. A practical heuristic for finding graph minors. *arXiv*, abs/1406.2741, 2014.
- Vicky Choi. Minor-embedding in adiabatic quantum computation: I. the parameter setting problem. *Quantum Information Processing*, 7(5):193–209, 2008.

- Vicky Choi. Minor-embedding in adiabatic quantum computation: II. minor-universal graph design. *Quantum Information Processing*, 10(3):343–353, 2011.
- Carleton Coffrin, Harsha Nagarajan, and Russell Bent. Evaluating ising processing units with integer programming. In Louis-Martin Rousseau and Kostas Stergiou, editors, *Integration of Constraint Programming, Artificial Intelligence, and Operations Research*, pages 163–181. Springer International Publishing, 2019.
- Don Coppersmith, David Gamarnik, and Maxim Sviridenko. The diameter of a long-range percolation graph. *Random Struct. Algorithms*, 21(1):1–13, 2002.
- D-Wave Systems. Introduction to the D-Wave Quantum Hardware. <https://www.dwavesys.com/tutorials/background-reading-series/introduction-d-wave-quantum-hardware>, 2019. Accessed: 2019-05-03.
- Prasanna Date, Robert Patton, Catherine Schuman, and Thomas Potok. Efficiently embedding qubo problems on adiabatic quantum computers. *Quantum Information Processing*, 18(4):117, 2019.
- Nike Dattani, Szilard Szalay, and Nick Chancellor. Pegasus: The second connectivity graph for large-scale quantum annealing hardware. *arXiv*, abs/1901.07636, 2019.
- Raouf Dridi, Hedayat Alghassi, and Sridhar Tayur. A novel algebraic geometry compiling framework for adiabatic quantum computations. *arXiv*, abs/1810.01440, 2018.
- Edward Farhi, Jeffrey Goldstone, Sam Gutmann, and Michael Sipser. Quantum computation by adiabatic evolution. *arXiv*, abs/quant-ph/0001106, 2000.
- Edward Farhi, Jeffrey Goldstone, Sam Gutmann, Joshua Lapan, Andrew Lundgren, and Daniel Preda. A quantum adiabatic evolution algorithm applied to random instances of an NP-complete problem. *Science*, 292(5516):472–475, 2001.
- AB Finnila, MA Gomez, C Sebenik, C Stenson, and JD Doll. Quantum annealing: A new method for minimizing multidimensional functions. *Chemical physics letters*, 219(5-6):343–348, 1994.

- Timothy D Goodrich, Eric Horton, and Blair D Sullivan. Practical graph bipartization with applications in near-term quantum computing. *arXiv*, abs/1805.01041, 2018a.
- Timothy D Goodrich, Blair D Sullivan, and Travis S Humble. Optimizing adiabatic quantum program compilation using a graph-theoretic framework. *Quantum Information Processing*, 17(5):118, 2018b.
- Kathleen E. Hamilton and Travis S. Humble. Identifying the minor set cover of dense connected bipartite graphs via random matching edge sets. *Quantum Information Processing*, 16(4):1–17, 2017.
- Tadashi Kadowaki and Hidetoshi Nishimori. Quantum annealing in the transverse ising model. *Physical Review E*, 58(5):5355, 1998.
- Bahman Kalantari. Quadratic functions with exponential number of local maxima. *Operations Research Letters*, 5(1):47–49, 1986.
- W. M. Kaminsky and S. Lloyd. Scalable architecture for adiabatic quantum computing of NP-hard problems. In A. J. Leggett, B. Ruggiero, and P. Silvestrini, editors, *Quantum Computing and Quantum Bits in Mesoscopic Systems*, pages 229–236. Springer US, Boston, MA, 2004.
- W. M. Kaminsky, S. Lloyd, and T. P. Orlando. Scalable superconducting architecture for adiabatic quantum computation. *arXiv*, abs/quant-ph/0403090, 2004.
- Hamed Karimi and Gili Rosenberg. Boosting quantum annealer performance via sample persistence. *Quantum Information Processing*, 16(7):166, 2017.
- Christine Klymko, Blair D Sullivan, and Travis S Humble. Adiabatic quantum programming: minor embedding with hard faults. *Quantum Information Processing*, 13(3):709–729, 2014.
- Andrew Lucas. Ising formulations of many np problems. *Frontiers in Physics*, 2:5, 2014.
- Andrew Lucas. Hard combinatorial problems and minor embeddings on lattice graphs. *arXiv*, abs/1812.01789, 2018.
- Catherine C. McGeoch and Cong Wang. Experimental evaluation of an adiabatic quantum system for combinatorial optimization. In *Proceedings of the ACM International Conference on Computing Frontiers*, CF '13, pages 23:1–23:11, 2013.

- Manfred Padberg. The boolean quadric polytope: Some characteristics, facets and relatives. *Mathematical Programming*, 45(1):139–172, 1989.
- Troels F. Rønnow, Zihui Wang, Joshua Job, Sergio Boixo, Sergei V. Isakov, David Wecker, John M. Martinis, Daniel A. Lidar, and Matthias Troyer. Defining and detecting quantum speedup. *Science*, 345(6195):420–424, 2014.
- W. Van Dam, M. Mosca, and U. Vazirani. How powerful is adiabatic quantum computation? In *Proceedings of the 42nd IEEE Symposium on Foundations of Computer Science*, FOCS '01, pages 279–287, 2001. ISBN 0-7695-1390-5.
- Z. Yang and M. J. Dinneen. Graph minor embeddings for d-wave computer architecture. Technical Report CDMTCS-503, Centre for Discrete Mathematics and Theoretical Computer Science, The University of Auckland, 2016.
- Arman Zaribafiyani, Dominic J. J. Marchand, and Seyed Saeed Changiz Rezaei. Systematic and deterministic graph minor embedding for cartesian products of graphs. *Quantum Information Processing*, 16(5), 2017.